Supporting information

Sustainable valorization of cherry (*Prunus avium* L.) pomace waste *via* the combined use of (NA)DESs and bio-ILs

Angelica Mero[1], Andrea Mezzetta[1,2], Marinella De Leo[1,2,3,#], Alessandra Braca[1,2,3], Lorenzo Guazzelli[1,2,#]

[1]Department of Pharmacy, Via Bonanno 33, 56126, Pisa, Italy

[2] Centre for Instrumentation Sharing, University of Pisa (CISUP), Lungarno Pacinotti 43, 56127 Pisa, Italy

[3] Interdepartmental Research Center Nutrafood "Nutraceuticals and Food for Health", University of Pisa, Via del Borghetto 80, 56124 Pisa, Italy

[#]corresponding author

Table of contents

Characterization methods

NMR Spectroscopy

^{1}H NMR spectra were recorded in D_2O or MeOD, on a Bruker 400 MHz NMR spectrometer at 25 °C. The experiments were performed using 50 mg/mL as sample concentration. ^{13}C NMR spectra were recorded at 101 MHz. ^{1}H and ^{13}C NMR chemical shifts (ppm) are referenced to the either residual D_2O (δ_H 4.79) or MeOD (δ_H 3.31, δ_C 49.0).

UHPLC-HR-ESI-MS analyses

The chemical characterization of all CPW extracts in terms of specialized metabolites was performed by means of UHPLC-HR-Orbitrap-ESI-MS (Q Exactive Plus MS, Thermo Fischer Scientific Inc., Germany). Methanolic solution (2 mg/mL) of all extracts were injected into the LC-MS system (5 µL injection volume) and analyzed on a C-18 Kinetex® Biphenyl column (100 x 2.1 mm, 2.6 µm particle size) provided of a Security Guard™ Ultra Cartridge (Phenomenex, Italy). For the elution formic acid in ACN 0.1% v/v (solvent A) and formic acid in H_2O 0.1% v/v (solvent B) were used developing a linear solvent gradient from 5 to 50% A within 11 min, at a flow rate 0.5 mL/min. For the anthocyanin analysis a linear solvent gradient from 5 to 20% A within 5 min was applied. The autosampler and column oven temperature was maintained at 4 and 35 °C, respectively. HR mass spectra were acquired in ESI negative ionization mode (scan range of *m/z* 120-1200) for phenol extracts and in positive ionization mode for the anthocyanin extracts, operating in full (70000 resolution, 220 ms maximum injection time) and data dependent-MS/MS scan (17500 resolution, 60 ms maximum injection time). Ionization parameters were optimized as follows: spray voltage 3500 V, capillary temperature 300 °C, sheath gas (N_2) 20 arbitrary unit, auxiliary gas (N_2) 3 arbitrary unit, collisionally activated dissociation (HCD) 18 eV, stepped normalized collisional energy (NCE) 20, 40, and 100%. Data were elaborated with Xcalibur 4.1 software. The quantitative amount of the major phenols identified in all extracts was determined by constructing calibration curves using chlorogenic acid, naringenin, rutin, and cyanidin 3-*O*-glucoside as external standards for quantification of hydroxycinnamic acids, flavonoid aglycones, flavonol *O*-glycosides, and anthocyanins, respectively. Stock methanol solutions were first prepared at 1 mg/mL concentration and successively diluted by serial dilution to obtain solutions at different concentrations in the following range: 0.001-200 µg/mL for chlorogenic acid, 0.5-50 µg/mL for naringenin and rutin, 25-250 µg/mL for cyanidin 3-*O*-glucoside. All solutions were prepared in triplicate. To construct calibration curves, the standard concentrations were plotted with respect to the areas obtained by MS peak integration. The relation between variables was obtained by linear simple correlation (R^2= 0.999 for chlorogenic acid; R^2 = 0.9782 for naringenin, R^2 = 0.9892 for rutin, and R^2= 0.9960 for cyanidin glucoside). The amounts of each component were finally expressed as µg/g ± standard deviation (SD) of dried cherry-waste. Data were obtained by Microsoft® Office Excel.

Fourier Transform Infrared Spectroscopy

The ATR-Fourier transform infrared spectroscopy (FTIR) spectra were recorded with an Agilent Technologies IR Cary 660 FTIR spectrophotometer using a macro-ATR accessory, a Diamond crystal. The spectra were measured in the range from 4000 to 500 cm^{-1} with 32 scans both for samples and background, measured first to eliminate the moisture and CO_2 from the samples.

Thermogravimetric analysis

Thermogravimetric analyses (TGA) were carried out using a TA Instruments Q500 TGA (weighing Precision ± 0.01%, sensitivity 0.1 mg, baseline dynamic drift < 50 mg). TG measurements were performed heating 5-15 mg of each sample at a rate of 10 °C min^{-1}, from 30 °C to 800 °C under nitrogen flow (80 cm^3 min^{-1}) in a platinum crucible. The instrument was calibrated using weight standards (1 g, 500 mg and 100 mg) and the temperature calibration was performed using curie point of nickel standard. All the standards were supplied by TA Instruments Inc. TGA experiments were carried out in triplicate.

Determination of chemical composition of biomass

-Water-soluble carbohydrate content

Free water-soluble sugar content was determined following the procedure reported by Saïed et al.[1] with slight modifications. More in detail, 1 g of CPW was treated with 50 mL of water at 90 °C for 30 min. The soluble fraction was recovered by filtration. The supernatant was evaporated under reduced pressure and the obtained sugars were analyzed by ^1H NMR (Figure S1). The test was performed in duplicate. The water-soluble sugars content was quoted as wt% of the dried biomass weight (calculated as g of water-soluble sugars/g of the dried biomass*100).

-Pectin content

Pectin content was determined using the procedure reported by Yang et al.[2] with slight modifications. More in detail, 500 mg of CPW obtained after the removal of free water-solubel sugars was mixed with water (1:15 w/v) and the pH was adjusted to 2 with citric acid. The resulting solution was heated at 90 °C for 60 min, and then centrifuged at 4000 rpm for 30 min. The supernatant was collected and three volumes (v/v) of absolute ethanol were added to reprecipitate pectin at 4 °C overnight. The pectin precipitate was collected by centrifugation and washed twice with 80% (v/v) ethanol. Finally, the pectin was dried in an oven at 100 °C. The test was performed in duplicate. The pectin content was quoted as wt% of the dried CPW weight (calculated as g of pectin/g of the dried CPW*100).

-Holocellulose content

Holocellulose content was determined based upon the delignifying procedures described by Yokoyama et al.[3]. More in detail, in a round bottom flask, 500 mg of residue, obtained after removal of free sugars and pectin, and 20 mL water were mixed and heated with stirring at 90°C. Then, a sodium chlorite solution (20

wt%, 5 mL) and 2 mL of glacial acetic acid were added. The addition of sodium chlorite solution and glacial acetic acid was repeated at 30, 60, and 90 min after the first addition. 2 h after the first addition, the round bottom flask was cooled in a cold-water bath. Glass microfibers filter was used to filter the reaction mixture. The residue, holocellulose, was washed with hot water (3 × 100 mL) and acetone (20 mL) and dried at 100° C. The test was performed in duplicate. The holocellulose content was quoted as wt% of the dried CPW weight (calculated as g of holocellulose/g of the dried CPW*100).

Rheological properties of ionogel

The rheological properties of ChLev based-ionogel were measured using a modular compact rheometer (MCR 302, Anton Paar, Turin, Italy) equipped with a plate–plate geometry (Ø = 5 cm) and a protective hood. All experiments were carried out at room temperature controlled by a water-cooled Peltier system (H-PTD200, Anton Paar). Oscillatory tests (amplitude sweep and frequency sweep) were performed to measure the storage modulus G' and the loss modulus G". At first, the amplitude sweep test was performed between 0.1 and 1 %, applying a constant frequency of 1 Hz to determine the correct value of shear strain within the linear viscoelastic region LVER required for the frequency sweep test. This latter test was carried out over a range of oscillation frequencies between 100 and 0.1 rad/s at 0.1% of shear strain. Then, to classify the gel as physical or chemical one and to determine its strenght, the dependence of the elastic modulus was calculated by a power-law model as follow:

$$G' = G_0 \cdot \omega^a \qquad \text{Eq. 1}$$

where G_0 ($Pa \cdot s^a$) is a constant representing the gel strength, i.e. the measurement of the elastic energy stored in a unit volume of the network, which is the intercept with the log G′-axis and defined mathematically by Eq. (2), and *a* is the slope of the log G′-log frequency curve, which is characteristic for each material[4,5].

$$G_0 = \lim_{\omega \to \infty} G'(\omega) \qquad \text{Eq. 2}$$

The parameter *a* indicates the behaviour of the gel in the plateau region in terms of the internal structure of the material related to the type of interactions present inside the material. Hence, if *a* is zero, the material exhibits a solid-like material behaviour typical of a "true gel" because it is formed by covalent interactions, while when $a > 0$, physical interactions are responsible for maintaining the gel-like structure[6].Finally, the complex viscosity was fitted to a power-law model, as follow:

$$\eta^* = q \cdot \omega^{p-1} \qquad \text{Eq. 3}$$

where q ($Pa \cdot s^p$) provides the resistance deformation at frequencies near to zero, and p is a parameter whose physical meaning is related to the behaviour of the material. The material presents a shear-thinning behaviour if "p" > 1 while the material shows a shear-thickening behaviour if "p" < 1.

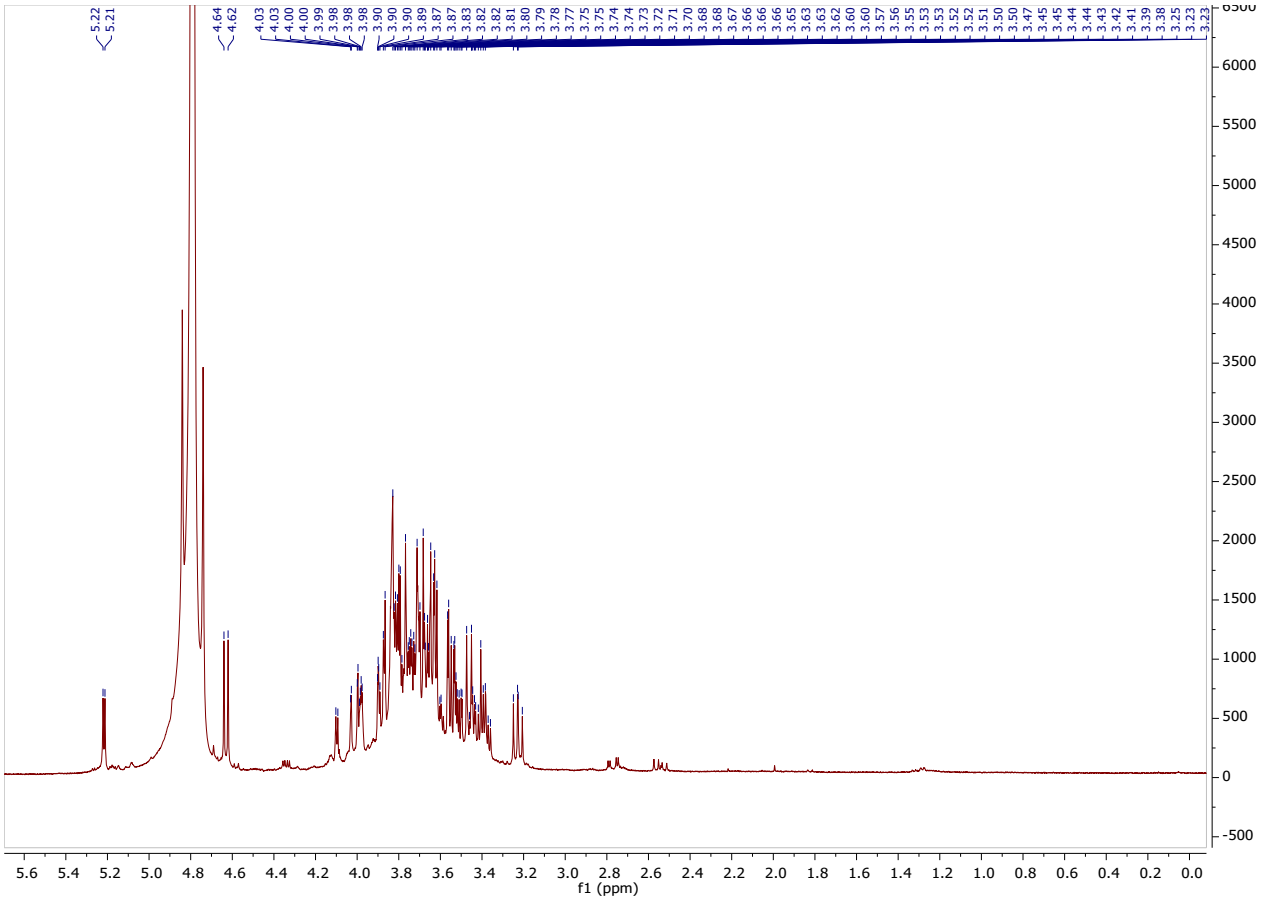

Figure S1. ^{1}H NMR of water-soluble sugars extracted from CPW.

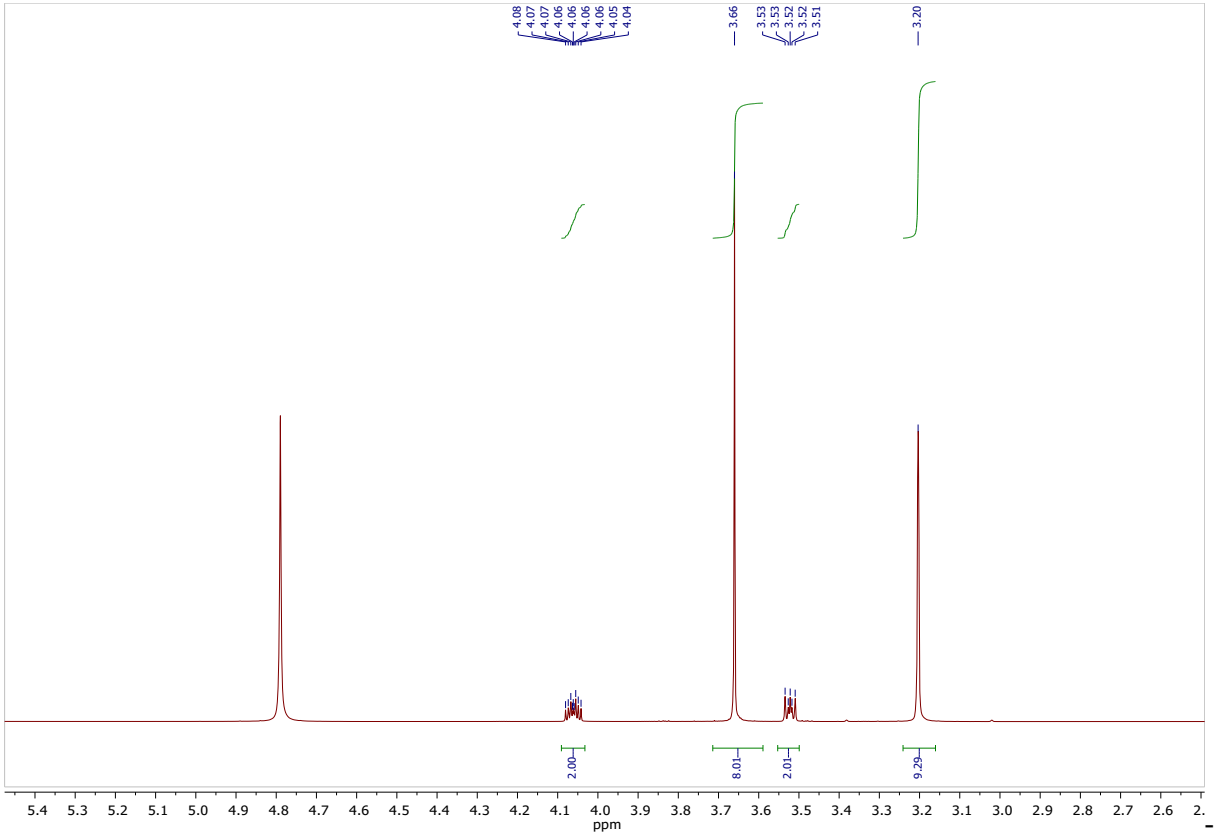

Figure S2. ^{1}H NMR of ChCl:EG 1:2 in D_2O.

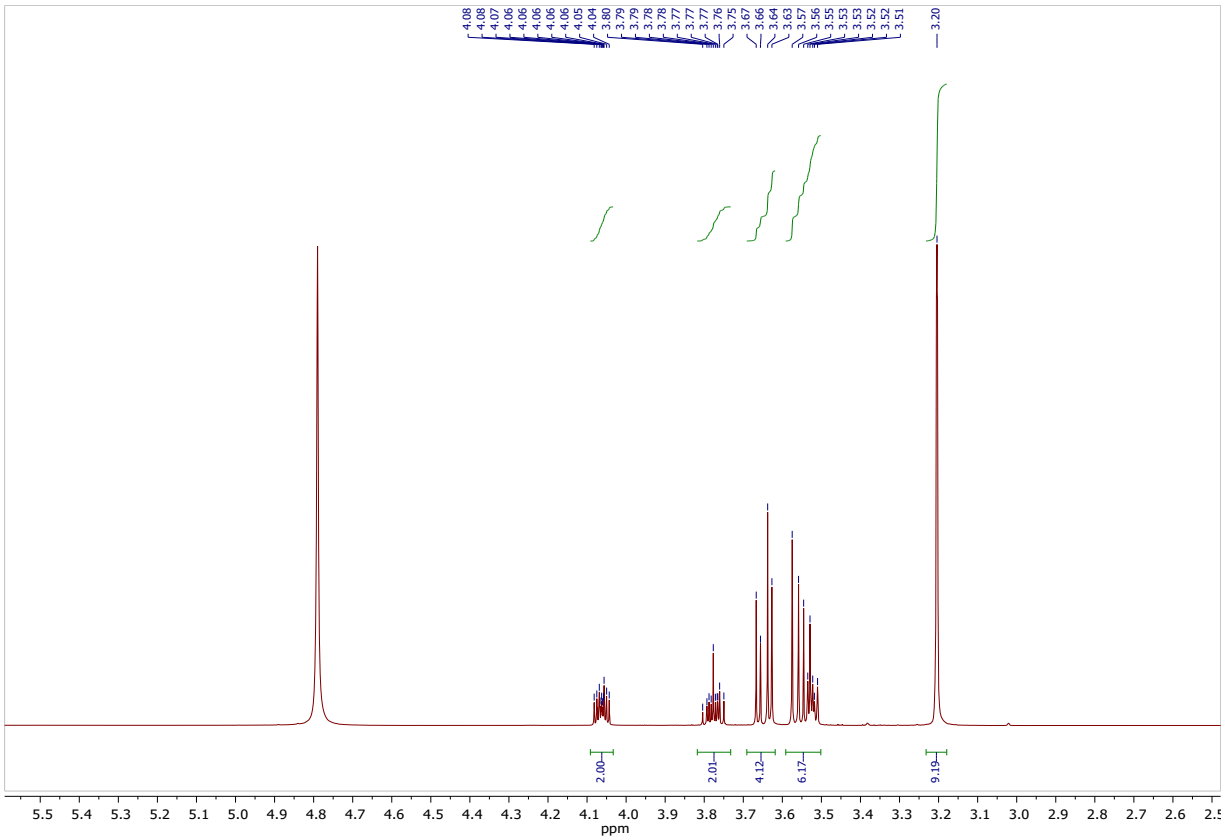

Figure S3. ^{1}H NMR of ChCl:Gly 1:2 in D_2O.

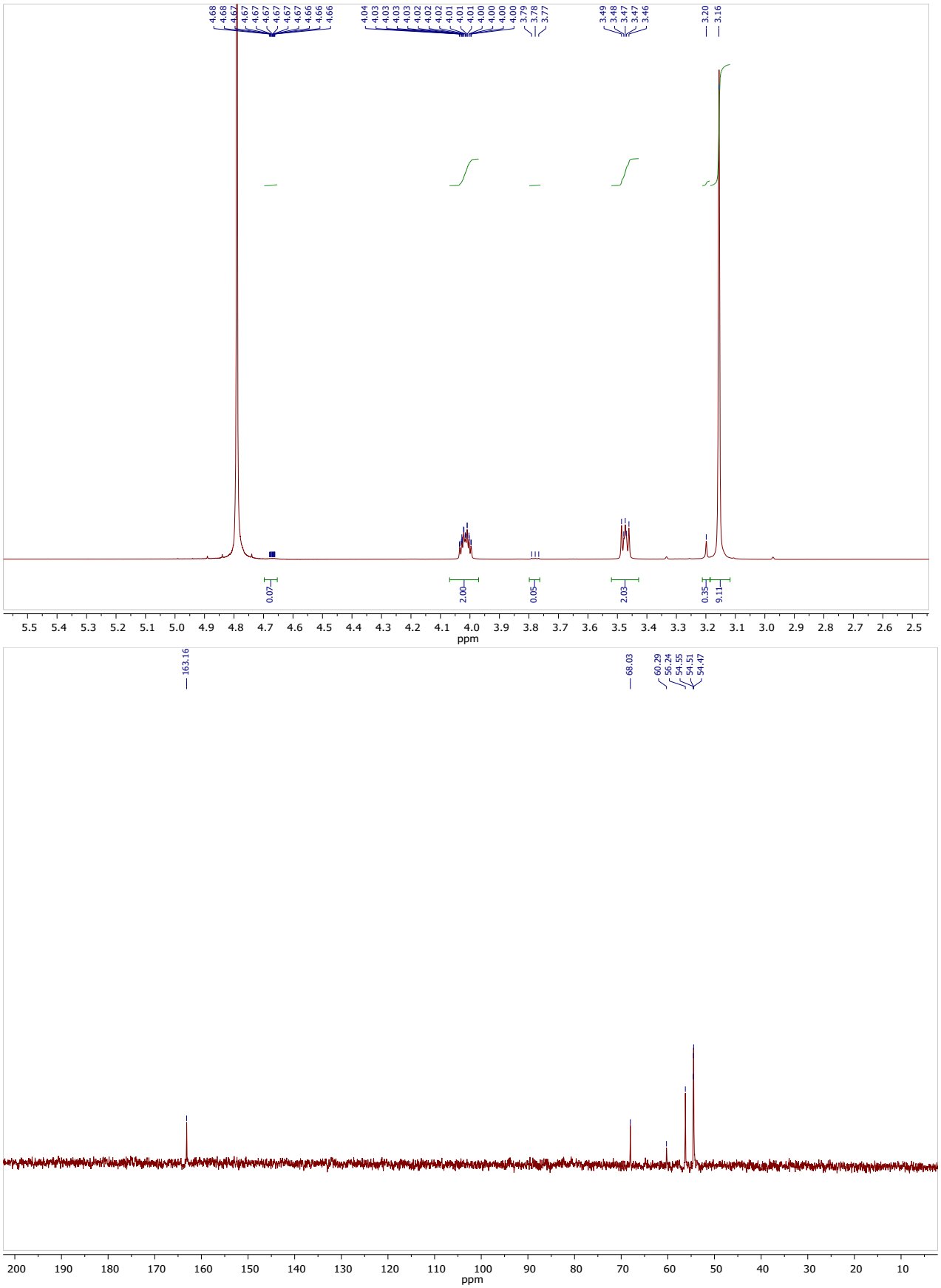

Figure S4. ^{1}H and ^{13}C NMR of ChCl:Oa 1:1 in D_2O.

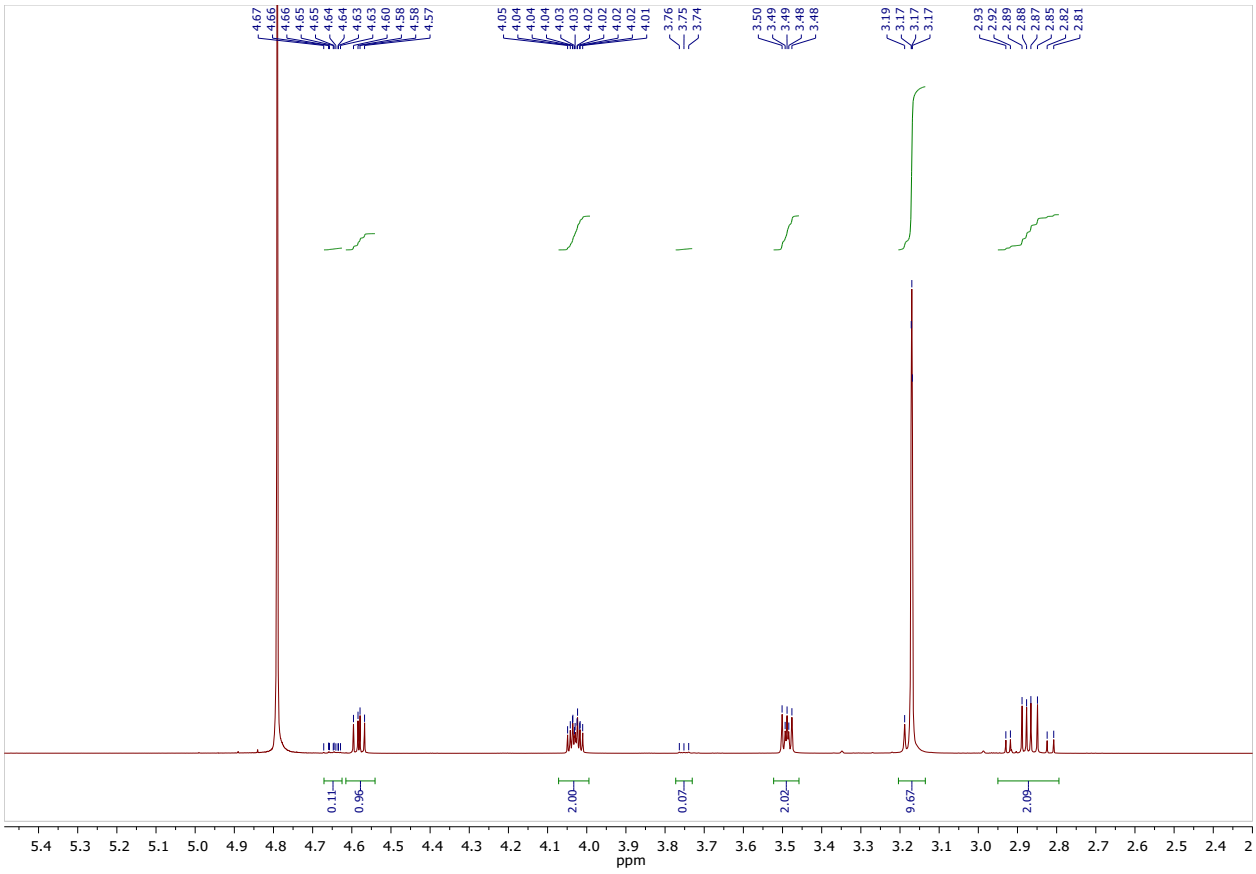

Figure S5. ^{1}H NMR of ChCl:Ma 1:1 in D_2O.

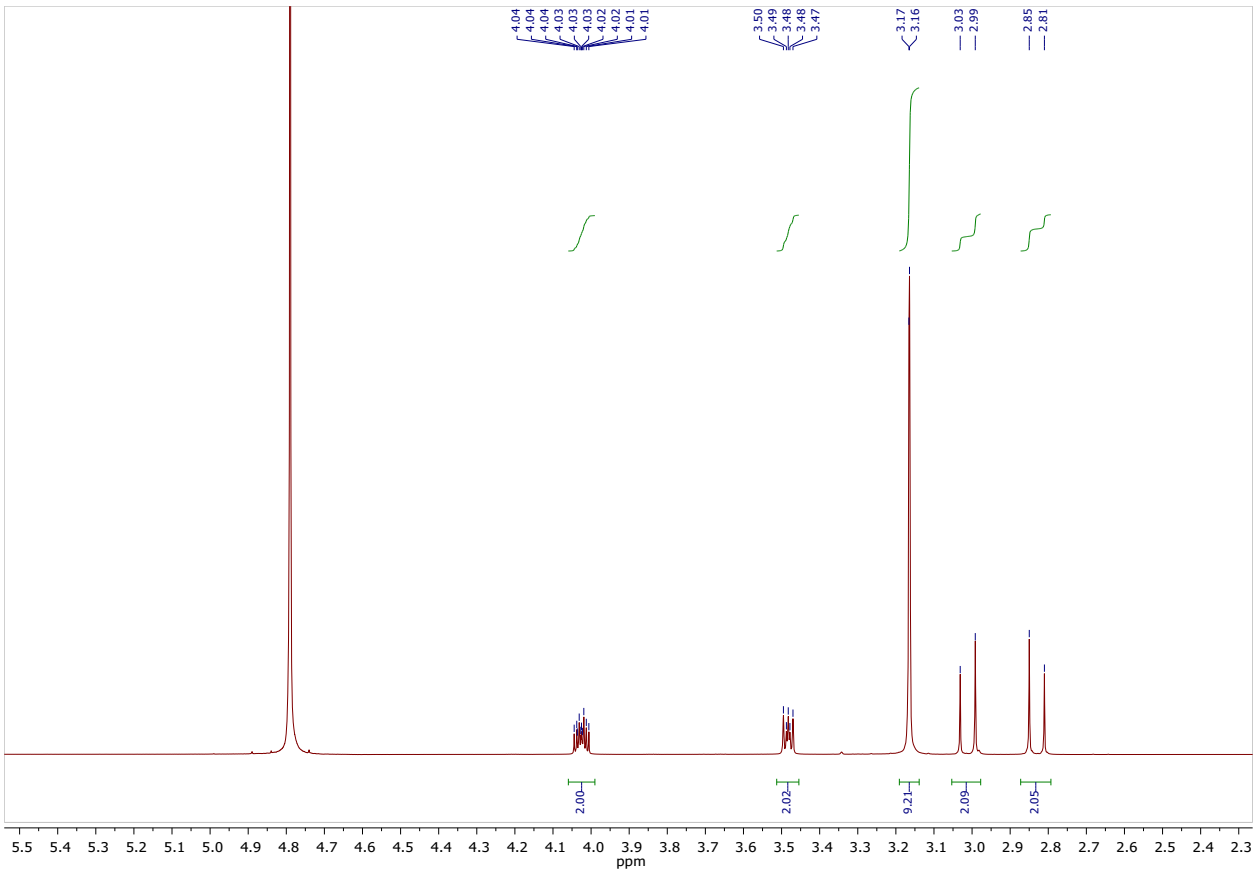

Figure S6. ^{1}H NMR of ChCl:CaxH_2O 1:1 in D_2O.

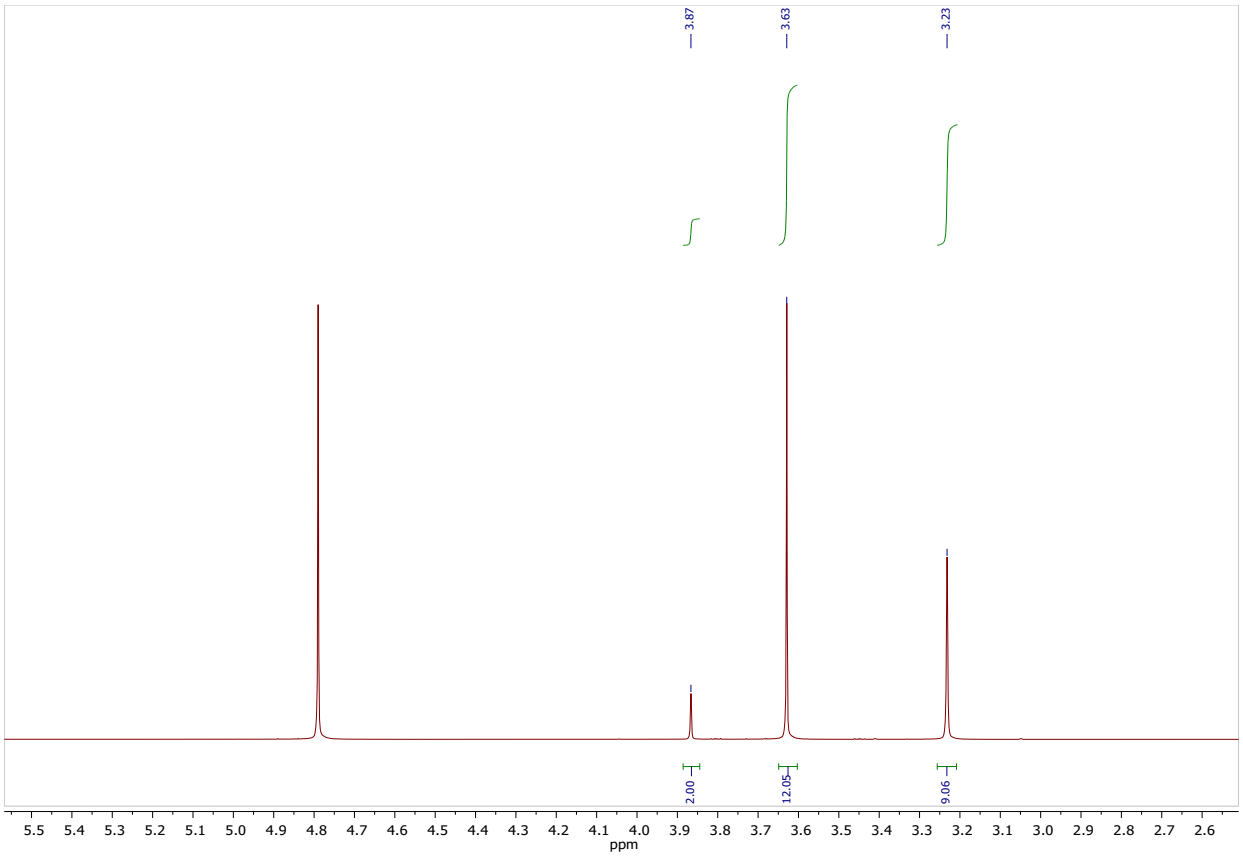

Figure S7. ^{1}H NMR of Bet:EG 1:3 in D_2O.

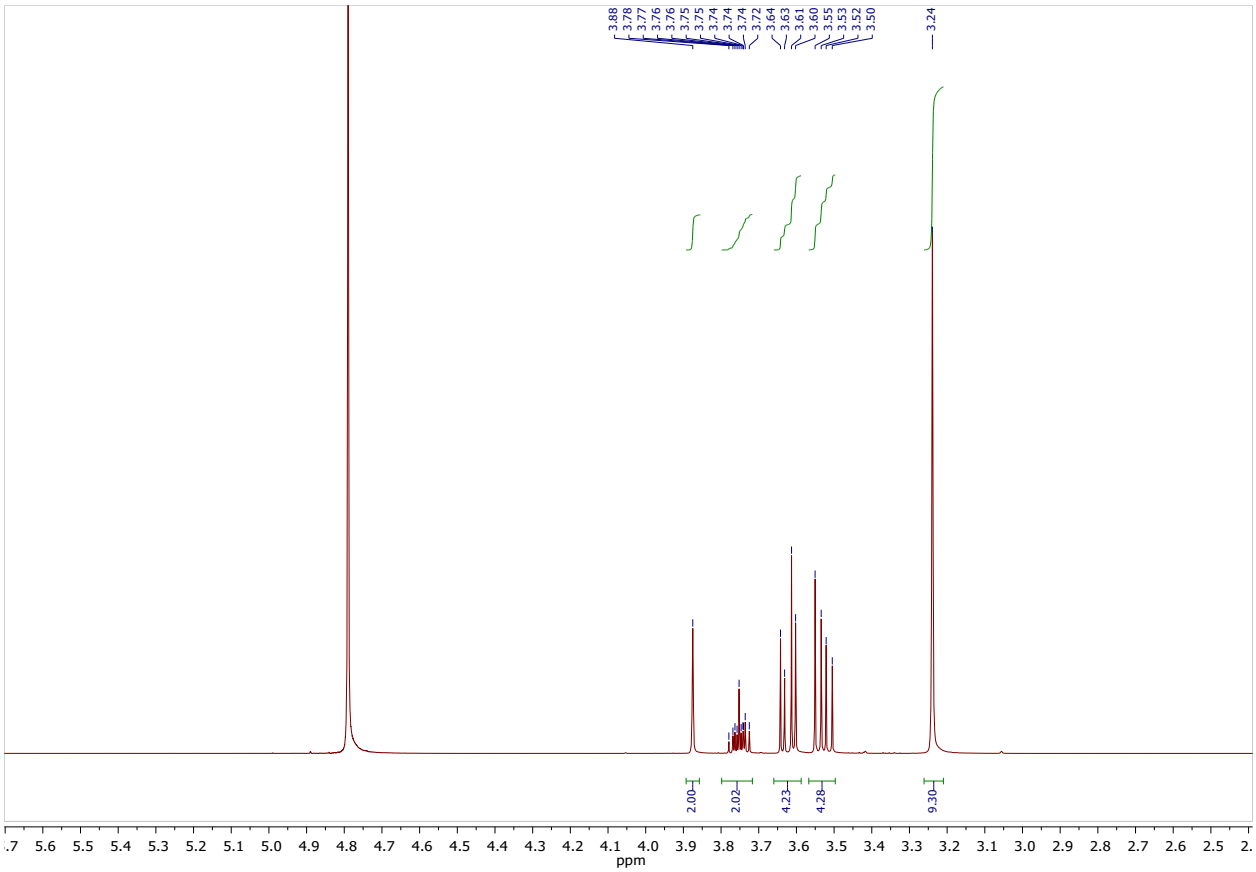

Figure S8. ^{1}H NMR of Bet:Gly 1:2 in D_2O.

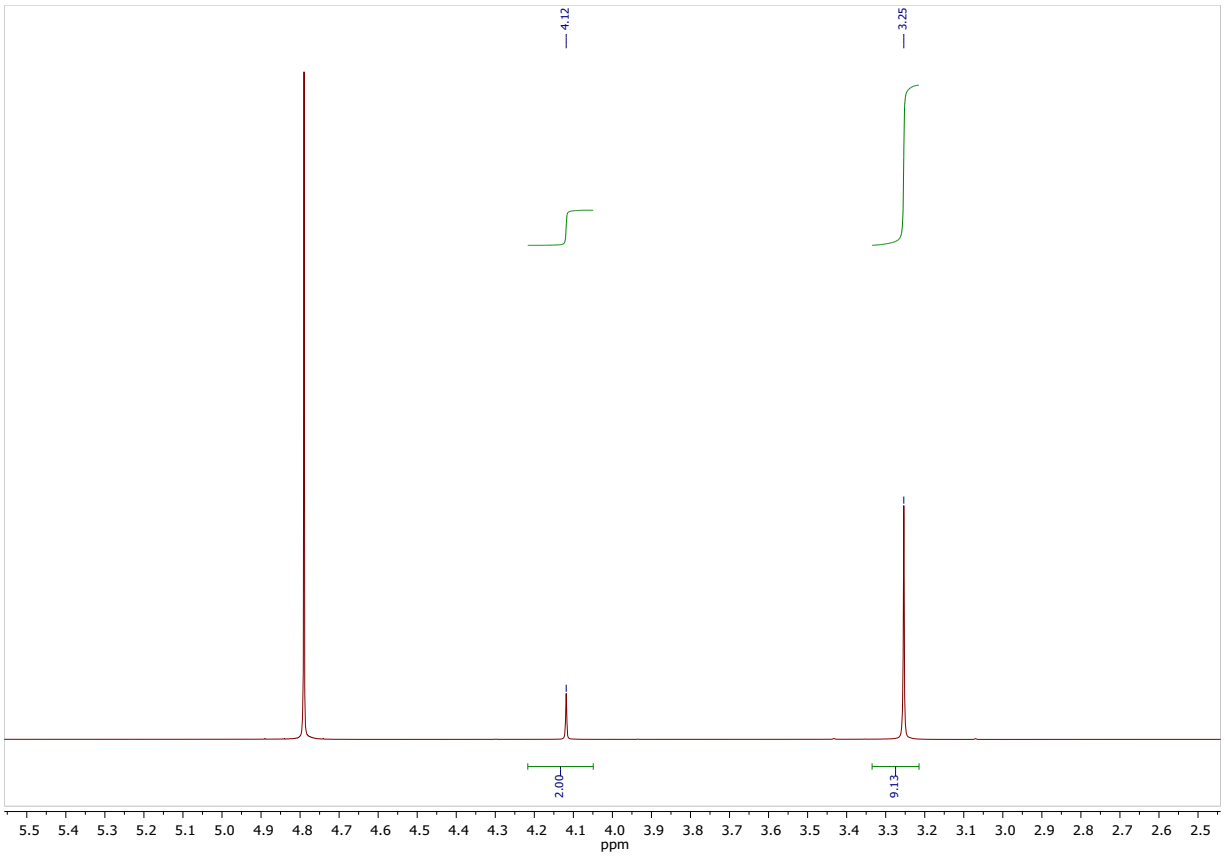

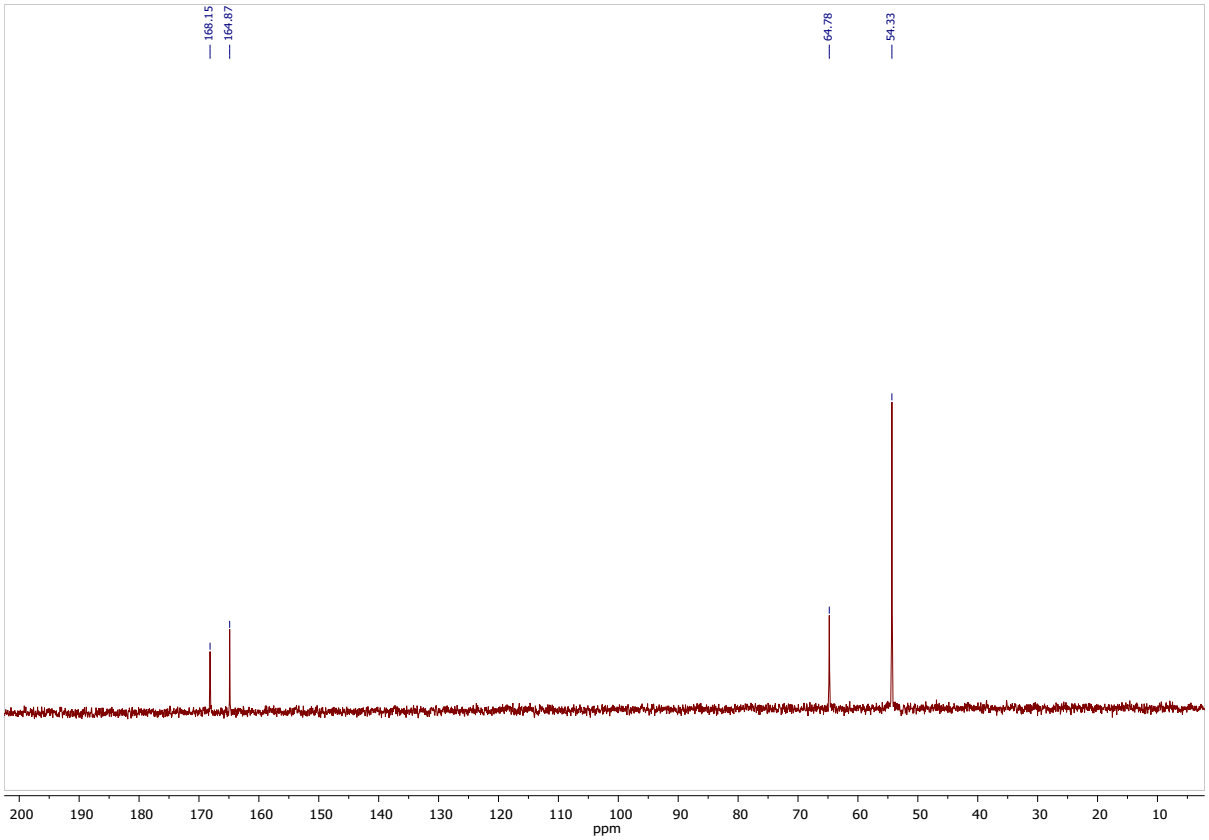

Figure S9. ^{1}H and ^{13}C NMR of Bet:Oa 1:1 in D_2O.

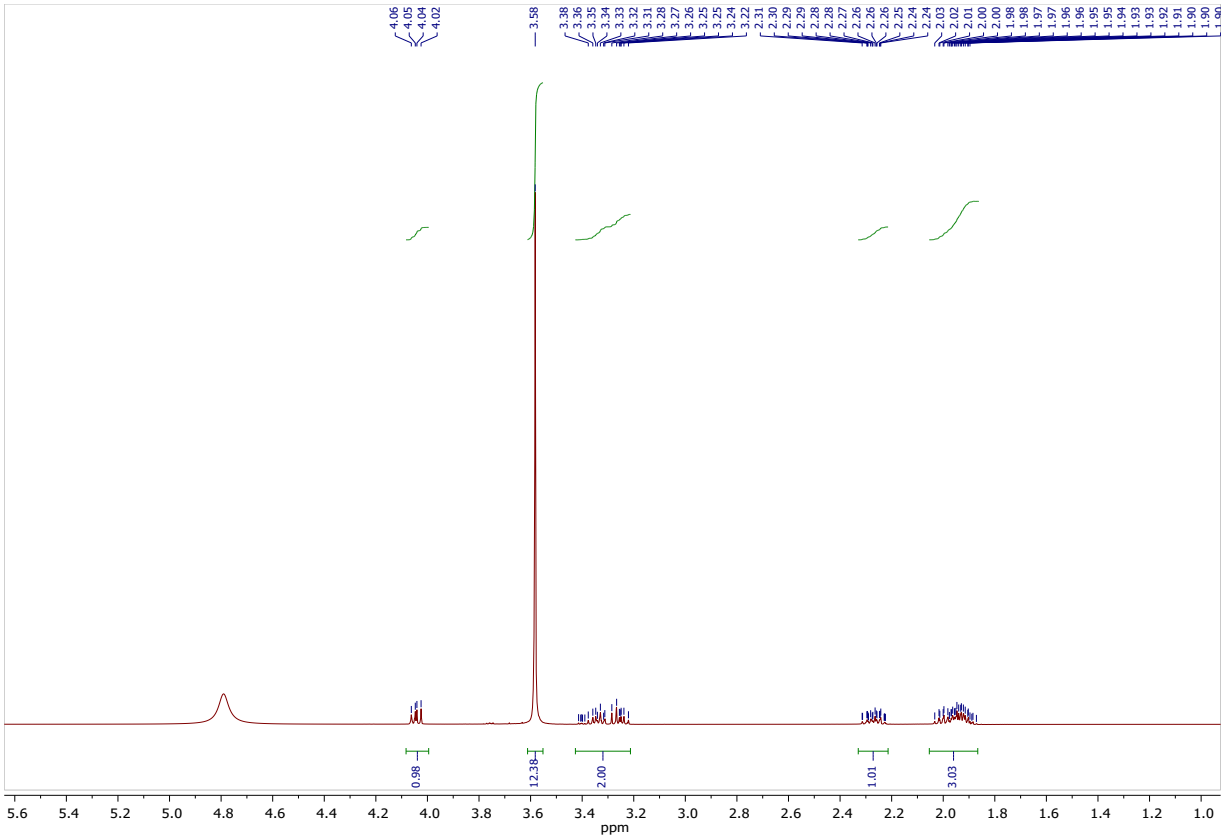

Figure S10. ^{1}H NMR of L-Pro:EG 1:3 in D_2O.

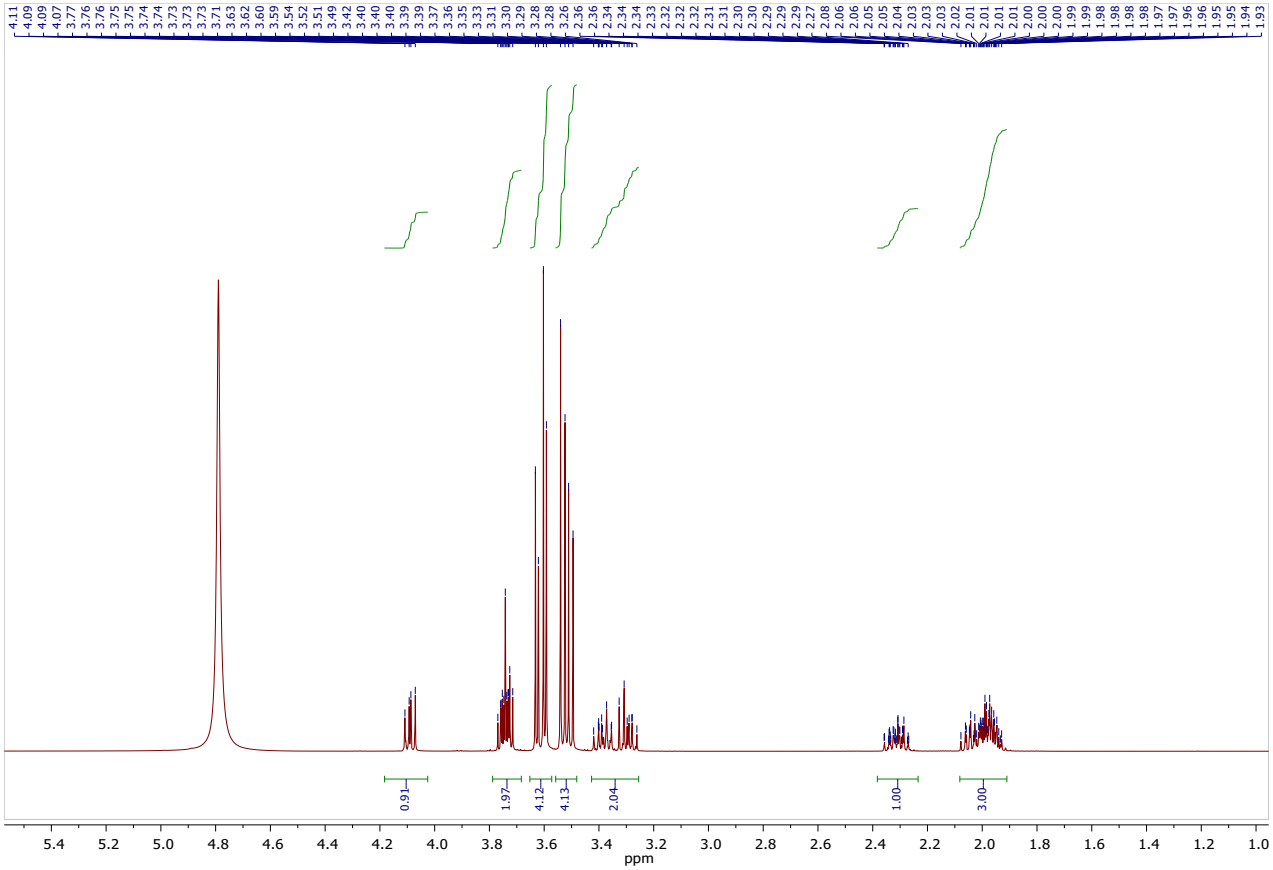

Figure S11. ^{1}H NMR of L-Pro:Gly 1:2 in D_2O.

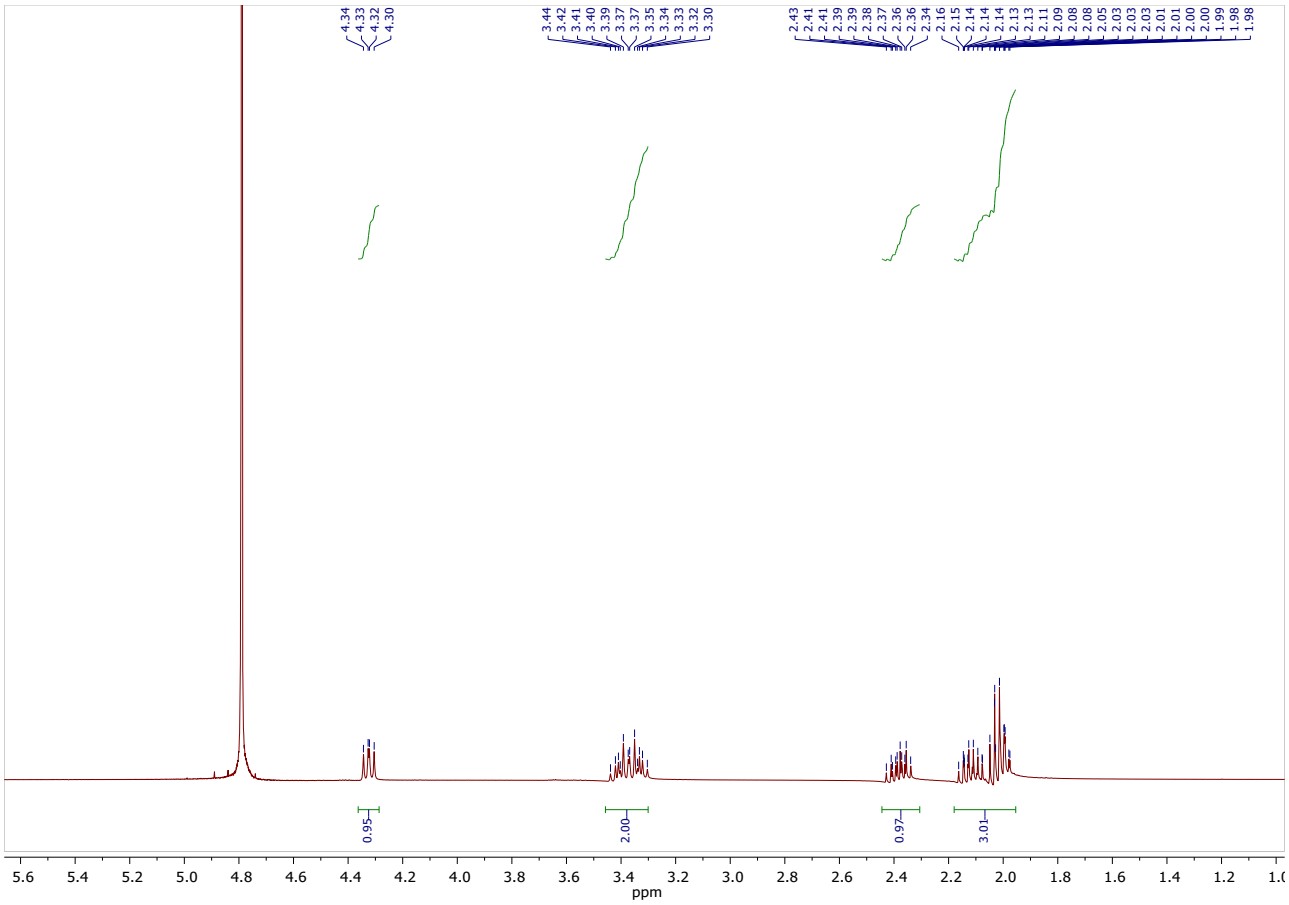
4.34
4.33
4.32
4.30
3.44
3.42
3.41
3.40
3.39
3.37
3.37
3.35
3.34
3.33
3.32
3.30
2.43
2.41
2.41
2.39
2.39
2.38
2.37
2.36
2.36
2.34
2.16
2.15
2.14
2.14
2.14
2.13
2.11
2.09
2.08
2.08
2.05
2.03
2.03
2.03
2.01
2.01
2.00
2.00
1.99
1.98
1.98
0.95
2.00
0.97
3.01
5.6 5.4 5.2 5.0 4.8 4.6 4.4 4.2 4.0 3.8 3.6 3.4 3.2 3.0 2.8 2.6 2.4 2.2 2.0 1.8 1.6 1.4 1.2
ppm

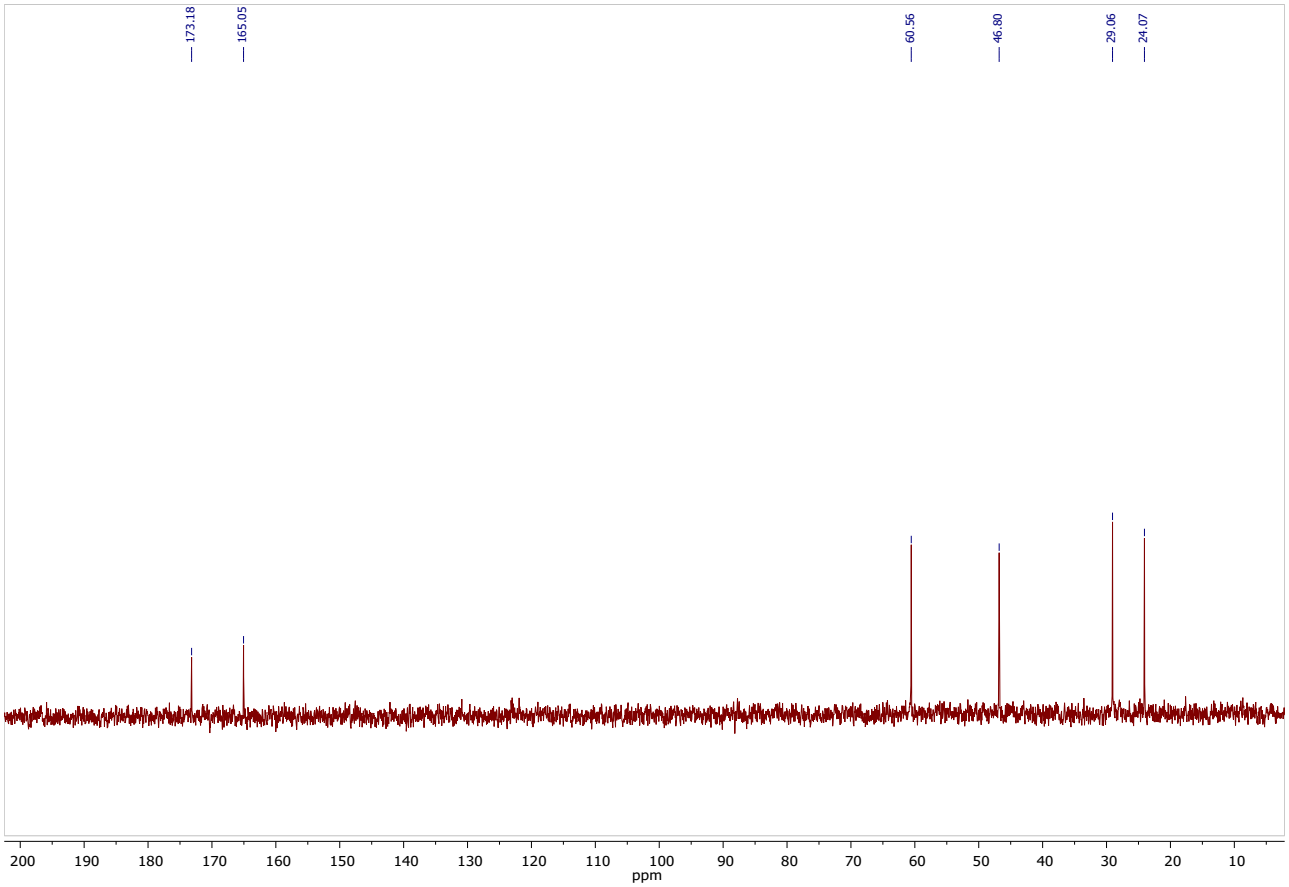
173.18
165.05
60.56
46.80
29.06
24.07
200 190 180 170 160 150 140 130 120 110 100 90 80 70 60 50 40 30 20 10
ppm

Figure S12. ^{1}H and ^{13}C NMR of L-Pro:Oa 1:1 in D_2O.

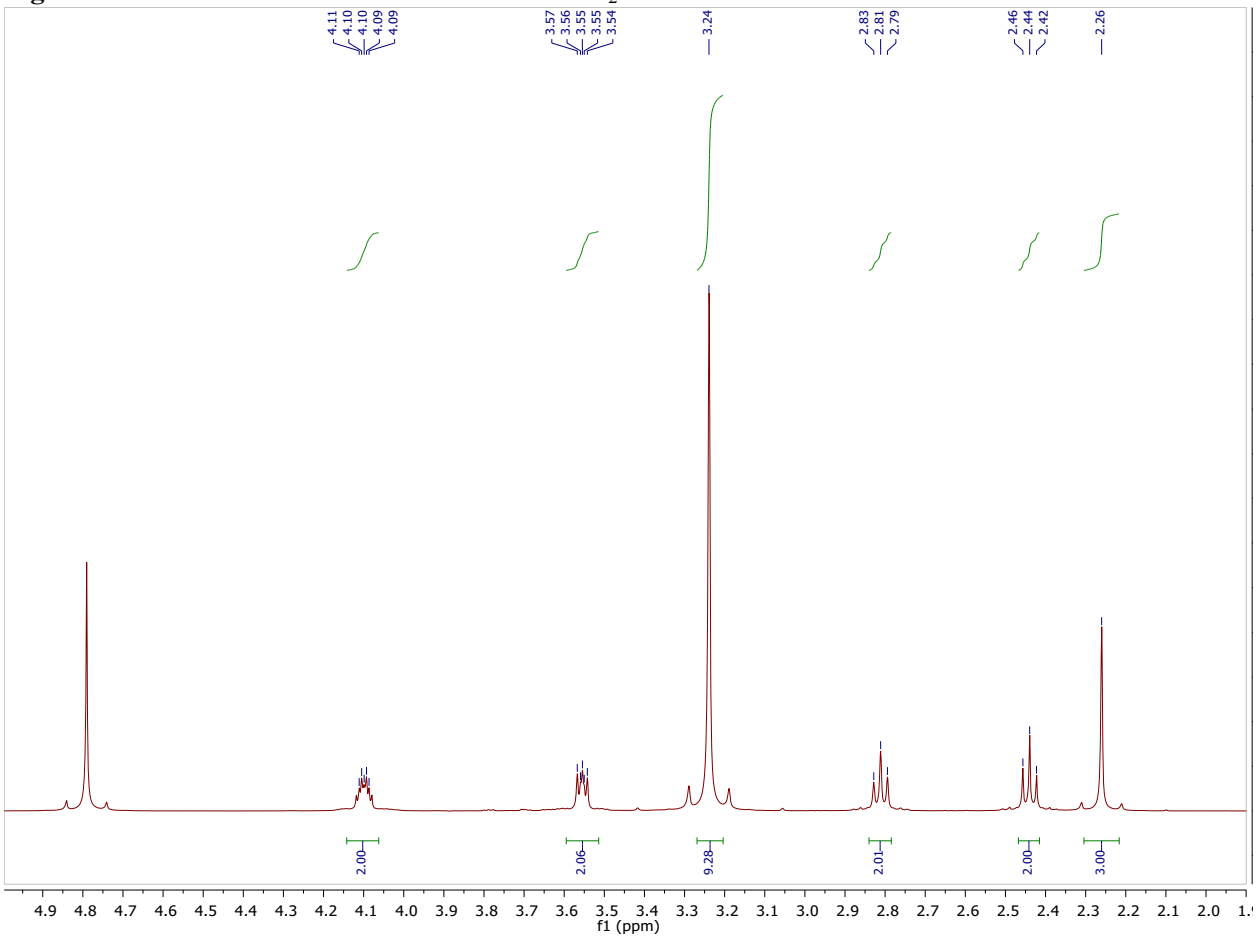

Figure S13. ^{1}H NMR of ChLev in D_2O.

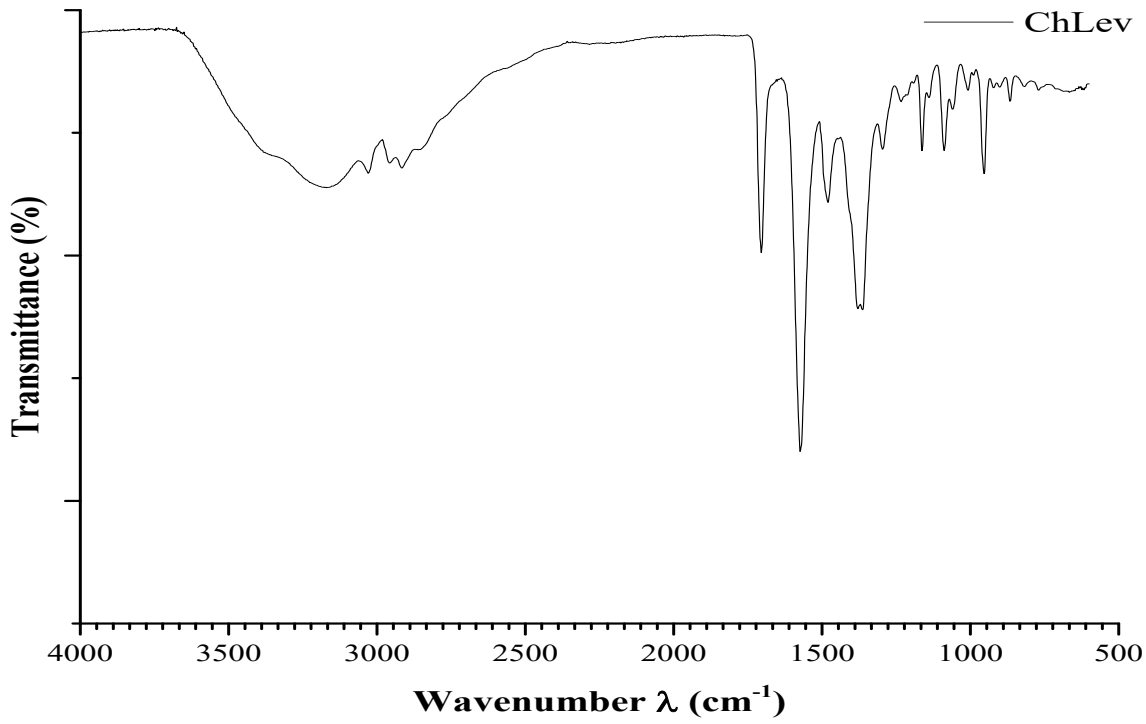

Figure S14. FTIR spectrum of ChLev.

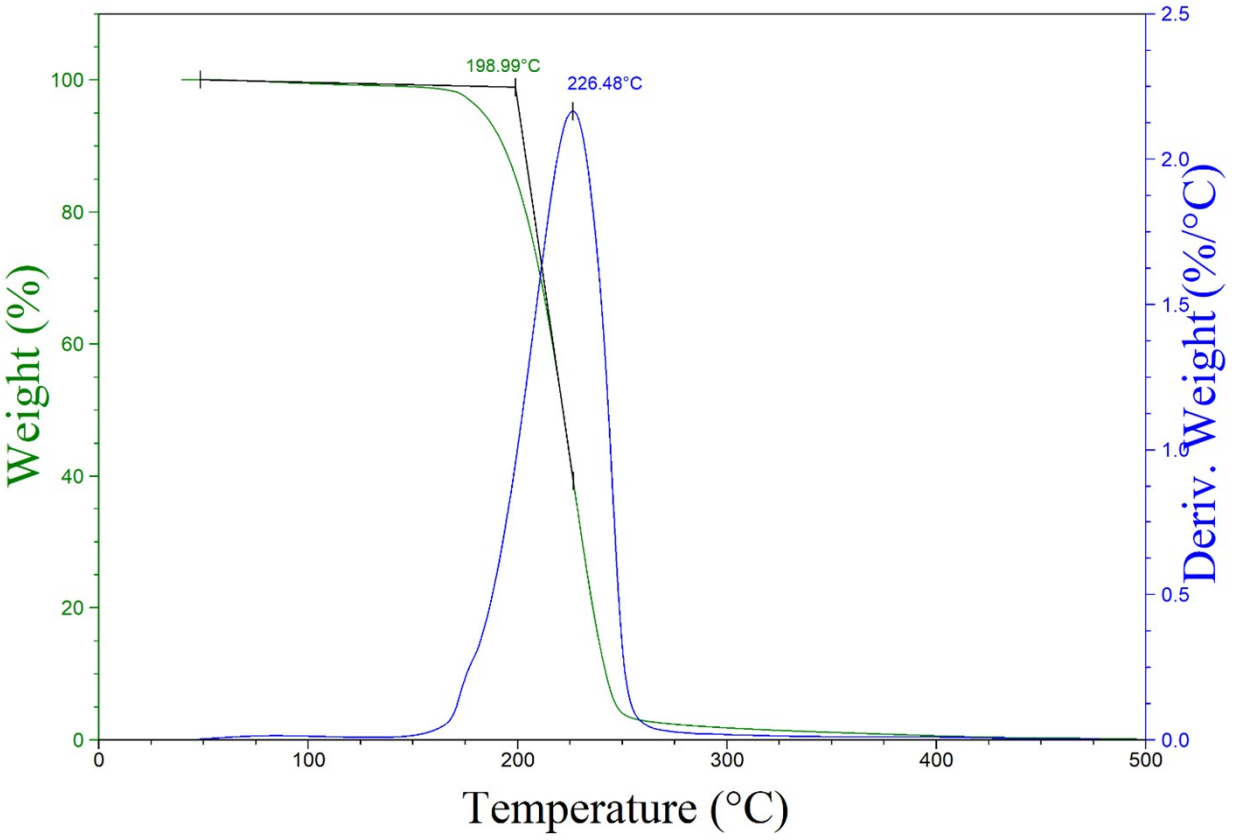

Figure S15. TG and DTG curves of ChLeV.

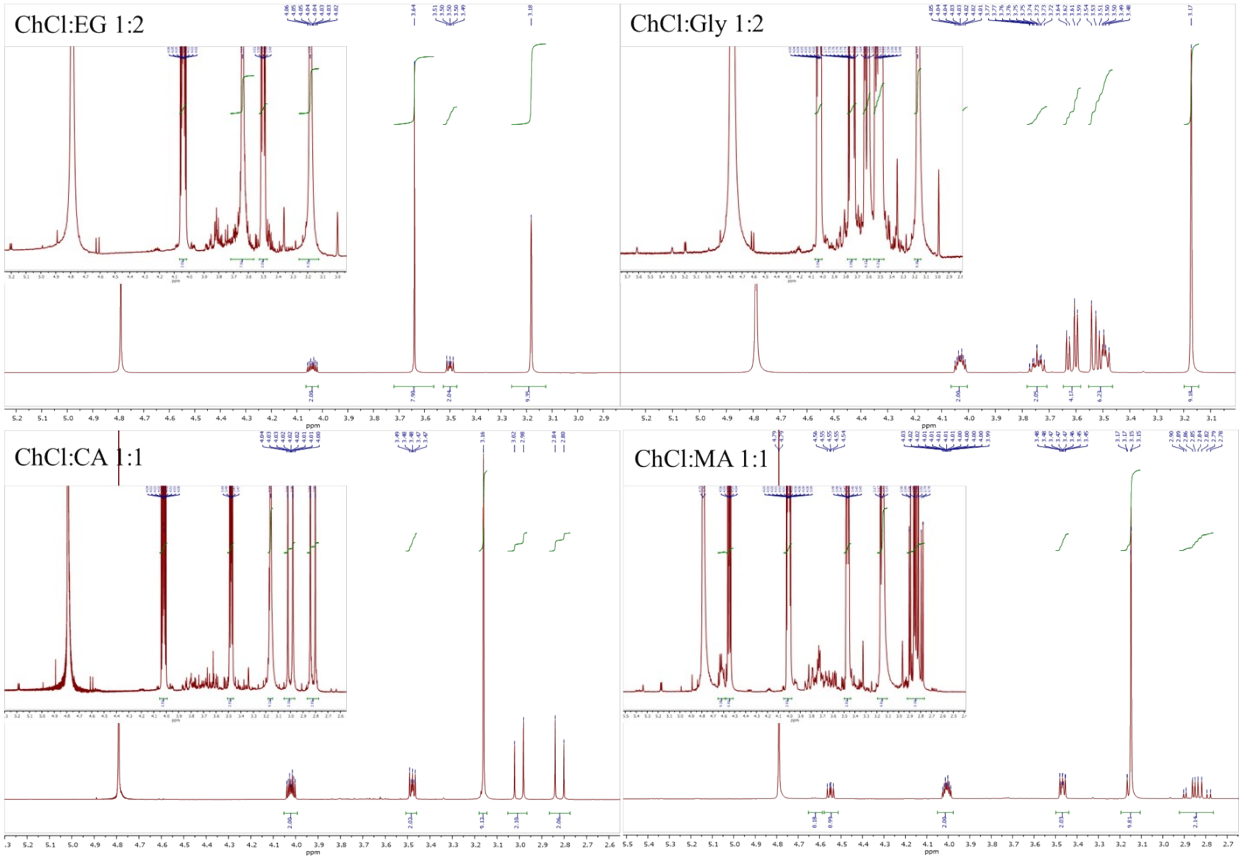

Figure S16. Some examples of ^{1}H NMR of recovered (NA)DESs after polyphenols extraction in D_2O and their enlargments.

Table S1. Amount (μg/g ± standard deviation of dried cherry pomace waste (CPW)) of phenols identified in six different CPW extracts obtained by classical solvents and (NA)DESs.

Peak	Compounds	*n*-BuOH	ChCl:EG	ChCl:Gly	ChCl:OA	ChCl:MA	ChCl:CA
	Phenolic acids						
1a, 1b	Dihydroxy benzoic acid (isomers I and II)	80.2 ± 3.6	179 ± 23	126 ± 18	271 ± 38	241 ± 3.9	85.6 ± 4.8
2	Chlorogenic acid	7.85 ± 0.44	8.32 ± 1.9	12.4 ± 0.97	19.4 ± 4.7	12.7 ± 0.43	4.40 ± 0.18
3a, 3b	3-*p*-Coumaroylquinic acid	24.6 ± 1.1	21.6 ± 4.7	46.8 ± 6.6	49.8 ± 9.2	0.0184 ± 0.29	11.0 ± 1.2
5a, 5b	3-*O*-Feruloylquinic acid (isomers *cis* and *trans*)	2.04 ± 0.13	7.42 ± 2.4	3.94 ± 0.59	4.73 ± 0.81	2.02 ± 0.098	1.09 ± 0.084
6a, 6b	4-*p*-Coumaroylquinic acid (isomers *cis* and *trans*)	4.04 ± 0.025	4.22 ± 1.1	13.7 ± 2.0	37.6 ± 6.2	19.8 ± 1.0	6.44± 0.61
	Flavonoid glycosides						
4	Kaempferol *O*-rutinoside	0.0231 ± 0.025	27.1 ± 7.2	5.30 ± 1.4	8.73 ± 2.3	19.4 ± 0.23	8.09 ± 0.23
7	Quercetin *O*-glucoside *O*-rutinoside	4.60 ± 0.27	15.6 ± 2.3	16.8 ± 2.1	4.65 ± 1.8	1.20 ± 0.12	2.52 ± 0.089
8	Kaempferol *O*-glucoside *O*-rutinoside	0.704 ± 0.040	2.28 ± 0.30	24.3 ± 0.34	0.61 ± 0.22	0.0810 ± 0.027	0.316 ± 0.051
9	Rutin	68.6 ± 5.3	131 ± 15	132 ± 18	32.9 ± 1.5	20.9 ± 0.70	26.5 ± 2.1
10	Apigenin *C*-glucoside	14.5 ± 0.42	31.3 ± 3.1	24.6 ± 3.6	25.3 ± 5.0	16.9 ± 0.55	9.24 ± 0.86
11	Quercetin *O*-glucoside	20.7 ± 0.88	30.0 ± 3.3	30.2 ± 3.8	6.00 ± 2.8	3.17 ± 0.077	3.91 ± 0.2
12	Kaempferol *O*-rutinoside	12.7 ± 0.38	21.7 ± 3.3	22.8 ± 2.4	5.71 ± 2.4	3.84 ± 0.086	4.51 ± 0.097
13	Kaempferol *O*-glucoside	6.64 ± 0.35	8.47 ± 0.83	9.85 ± 1.2	2.91 ± 1.7	0.938 ± 0.12	1.28 ± 0.11
15a, 15b	Naringenin *O*-hexoside I	5.58 ± 0.32	21.6 ± 3.1	7.56 ± 0.87	3.24 ± 1.9	0.019 ± 0.017	1.14 ± 0.13
17	Chrysin *O*-glucoside	25.5 ± 1.1	0.133 ± 0.027	48.8 ± 4.8	3.45 ± 0.63	2.43 ± 0.066	1.23 ± 0.16
18a, 18b	Naringenin *O*-hexoside II	12.0 ± 0.74	21.5 ± 2.2	12.9 ± 1.6	9.50 ± 1.8	4.25 ± 0.27	4.14 ± 0.19
22	Dihydrowogonin 7-*O*-β-D-glucopyranoside	3.70 ± 0.10	6.88 ± 0.89	6.44 ± 0.092	5.41 ± 3.9	1.78 ± 0.081	2.02 ± 0.13
	Flavonoid aglycones						
14	Aromadendrin	7.63 ± 0.23	5.31 ± 0.50	5.79 ± 0.64	0.632 ± 0.053	0.513 ± 0.016	0.302 ± 0.070
16	Quercetin	11.1 ± 0.62	19.3 ± 3.2	2.58 ± 0.11	1.67 ± 0.48	27.9 ± 0.91	3.85 ± 0.40
19	Naringenin	4.28 ± 0.28	5.03 ± 0.61	2.52 ± 0.38	4.91 ± 0.61	2.84 ± 0.076	2.20 ± 0.17
20	Apigenin	11.2 ± 0.31	15.2 ± 1.6	9.00 ± 1.1	4.62 ± 1.2	4.41 ± 0.070	2.58 ± 0.16
21	Naringenin isomer	8.88 ± 0.31	5.95 ± 0.67	6.34 ± 0.79	0.630 ± 0.35	0.618 ± 0.017	2.48 ± 0.17
23	Chrysin	34.1 ± 0.24	75.2 ± 8.0	22.1 ± 4.3	36.9 ± 6.4	32.0 ± 0.57	17.1 ± 0.73
24	Dihydrowogonin	13.8 ± 0.92	20.6 ± 2.7	9.18 ± 1.6	5.66 ± 2.0	3.61 ± 0.17	4.09 ± 0.17
	Anthocyanins	MeOH-HCl					
25	Cyanidin 3-*O*-rutinoside	0.43 ± 0.046	96.8 ± 6.8	28.3 ± 4.9	29.2 ± 4.0	65.0 ± 3.9	41.6 ± 4.3
26	Cyanidin 3-*O*-glucoside	5.28 ± 0.99	6.68 ± 0.29	1.09 ± 0.24	9.14 ± 0.92	20.8 ± 2.3	3.72 ± 0.75
	Total phenolic acids	119 ± 5.3	221 ± 33	203 ± 28	382 ± 59	275 ± 41	108 ± 6.9
	Total flavonoid glycosides	175 ± 9.9	318 ± 32	320 ± 40	108 ± 26	75.0 ± 2.3	64.9 ± 4.3
	Total flavonoid aglycones	67.9 ± 1.8	117 ± 13	46.6 ± 7.8	47.8 ± 9.9	40.6 ± 0.82	26.3 ± 1.2
	Total anthocyanins	5.71 ± 1.0	103 ± 7.1	29.4 ± 5.1	38.3 ± 4.9	85.8 ± 6.2	45.3 ± 5.0
	Total phenols	368 ± 18	759 ± 85	599 ± 81	576 ± 99	495 ± 15	245 ± 17

Peak numbers correspond to those of Figure 3.

Table S2. Amount (μg/g ± standard deviation of dried cherry pomace waste (CPW)) of phenols identified in six different CPW extracts obtained by (NA)DESs.

Peak	Compounds	L-Pro:EG	L-Pro:Gly	L-Pro:OA	Bet:EG	Bet:Gly	Bet:OA
	Phenolic acids						
1a, 1b	Dihydroxy benzoic acid (isomers I and II)	118 ± 11	108 ± 6.7	118 ± 7.8	145 ± 30	122 ± 1.9	115 ± 9.1
2	Chlorogenic acid	5.14 ± 0.35	1.83 ± 0.12	2.44 ± 0.29	2.37 ± 0.53	0.737 ± 0.048	3.77 ± 0.16
3a, 3b	4-*p*-Coumaroylquinic acid	10.7 ± 0.81	3.30 ± 0.33	1.34 ± 0.053	6.59 ± 1.3	1.66 ± 0.020	6.4 ± 0.52
5a, 5b	3-*O*-Feruloylquinic acid (isomers *cis* and *trans*)	8.80 ± 1.2	4.92 ± 0.23	12.4 ± 0.98	4.67 ± 1.2	6.17 ± 0.35	14.0 ± 0.88
6a, 6b	5-*p*-Coumaroylquinic acid (isomers *cis* and *trans*)	8.82 ± 0.94	5.01 ± 1.0	3.26 ± 0.12	5.71 ± 1.4	1.93 ± 0.12	6.23 ± 0.47
	Flavonoid glycosides						
4	Kaempferol *O*-rutinoside	2.85 ± 0.42	0.763 ± 0.093	6.52 ± 0.86	1.84 ± 0.44	0.937 ± 0.024	8.36 ± 1.1
7	Quercetin *O*-glucoside *O*-rutinoside	2.38 ± 0.21	0.238 ± 0.035	0.240 ± 0.058	1.69 ± 0.37	0.241 ± 0.012	0.709 ± 0.037
8	Kaempferol *O*-glucoside *O*-rutinoside	0.306 ± 0.043	0.00744 ± 0.0076	0.00267 ± 0.0046	0.209 ± 0.063	0.0147 ± 0.0062	0.101 ± 0.0043
9	Rutin	28.3 ± 2.2	4.21 ± 0.52	5.59 ± 0.57	19.0 ± 4.7	4.62 ± 0.15	13.8 ± 1.0
10	Apigenin *C*-glucoside	13.3 ± 1.1	10.5 ± 0.61	9.07 ± 0.68	13.2 ± 3.0	9.60 ± 0.38	11.4 ± 0.069
11	Quercetin *O*-glucoside	4.99 ± 0.44	0.701 ± 0.12	0.790 ± 0.11	3.38 ± 0.80	0.698 ± 0.0028	2.48 ± 0.14
12	Kaempferol *O*-rutinoside	4.84 ± 0.28	0.764 ± 0.064	0.942 ± 0.051	3.15 ± 0.68	0.823 ± 0.038	2.58 ± 0.22
13	Kaempferol *O*-glucoside	1.42 ± 0.13	0.213 ± 0.0059	0.227 ± 0.031	1.10 ± 0.22	0.229 ± 0.017	0.686 ± 0.039
15a, 15b	Naringenin *O*-hexoside I	1.37 ± 0.05	0.660 ± 0.028	0.437 ± 0.030	1.03 ± 0.24	0.378 ± 0.035	0.785 ±0.049
17	Chrysin *O*-glucoside	1.96 ± 0.16	1.51 ± 0.11	1.13 ± 0.079	1.93 ± 0.47	1.30 ± 0.045	1.64 ± 0.087
18a, 18b	Naringenin *O*- hexoside II	4.47 ± 0.29	1.40 ± 0.0068	1.35 ± 0.048	4.21 ± 0.90	1.24 ± 0.0078	2.04 ± 0.072
22	Dihydrowogonin 7-*O*-β-D-glucopyranoside	1.52 ± 0.081	0.912 ± 0.062	0.628 ± 0.048	1.69 ± 0.34	0.909 ± 0.05	0.685 ± 0.015
	Flavonoid aglycones						
14	Aromadendrin	1.28 ± 0.085	0.181 ± 0.0045	0.076 ± 0.0053	0.378 ± 0.088	0.0963 ± 0.0039	0.587 ± 0.033
16	Quercetin	10.8 ± 0.012	6.42 ± 0.19	3.51 ± 0.28	6.96 ± 1.7	4.00 ± 0.21	22.6 ± 1.9
19	Naringenin	1.72 ± 0.075	1.32 ± 0.051	0.959 ± 0.074	1.60 ± 0.37	1.13 ± 0.017	1.67 ± 0.10
20	Apigenin	4.35 ± 0.33	1.85 ± 0.13	1.99 ± 0.21	3.42 ± 0.66	1.770 ± 0.035	3.14 ± 0.20
21	Naringenin isomer	0.961 ± 0.048	0.522 ± 0.024	0.478 ± 0.027	0.600 ± 0.057	0.255 ± 0.0065	0.587 ± 0.031
23	Chrysin	26.2 ± 2.2	13.4 ± 0.74	14.9 ± 1.2	25.2 ± 0.13	13.2 ± 0.67	18.3 ± 1.8
24	Dihydrowogonin	4.13 ± 0.44	1.5 ± 0.40	1.15 ± 0.14	3.11 ± 0.64	1.51 ± 0.0028	2.31 ± 0.48
	Anthocyanins	MeOH-HCl					
25	Cyanidin 3-*O*-rutinoside	10.3 ± 0.91	2.95 ± 0.051	22.8 ± 2.2	5.96 ± 1.4	3.12 ± 0.25	27.1 ± 1.6
26	Cyanidin 3-*O*-glucoside	2.56 ± 0.21	1.95 ± 0.039	13.9 ± 0.93	1.2 ± 0.24	1.49 ± 0.096	11.7 ± 0.57
	Total phenolic acids	151 ± 14	123 ± 8.4	137 ± 9.2	164 ± 7.4	132 ± 2.4	145 ± 11
	Total flavonoid glycosides	67.7 ± 5.4	21.9 ± 1.7	26.9 ± 2.6	52.4 ± 9.1	21.0 ± 0.79	45.3 ± 3.4
	Total flavonoid aglycones	35.6 ± 3.0	17.3 ± 1.3	18.5 ± 1.7	32.4 ± 1.5	16.7 ± 0.71	24.3 ± 2.5
	Total anthocyanins	12.9 ± 1.1	4.90 ± 0.090	36.7 ± 3.1	7.16 ± 1.6	4.61 ± 0.35	38.8 ± 2.17
	Total phenols	267 ± 24	167 ± 11	219 ± 16	256 ± 19	175 ± 4.2	254 ± 19

Peak numbers correspond to those of Figure 3.

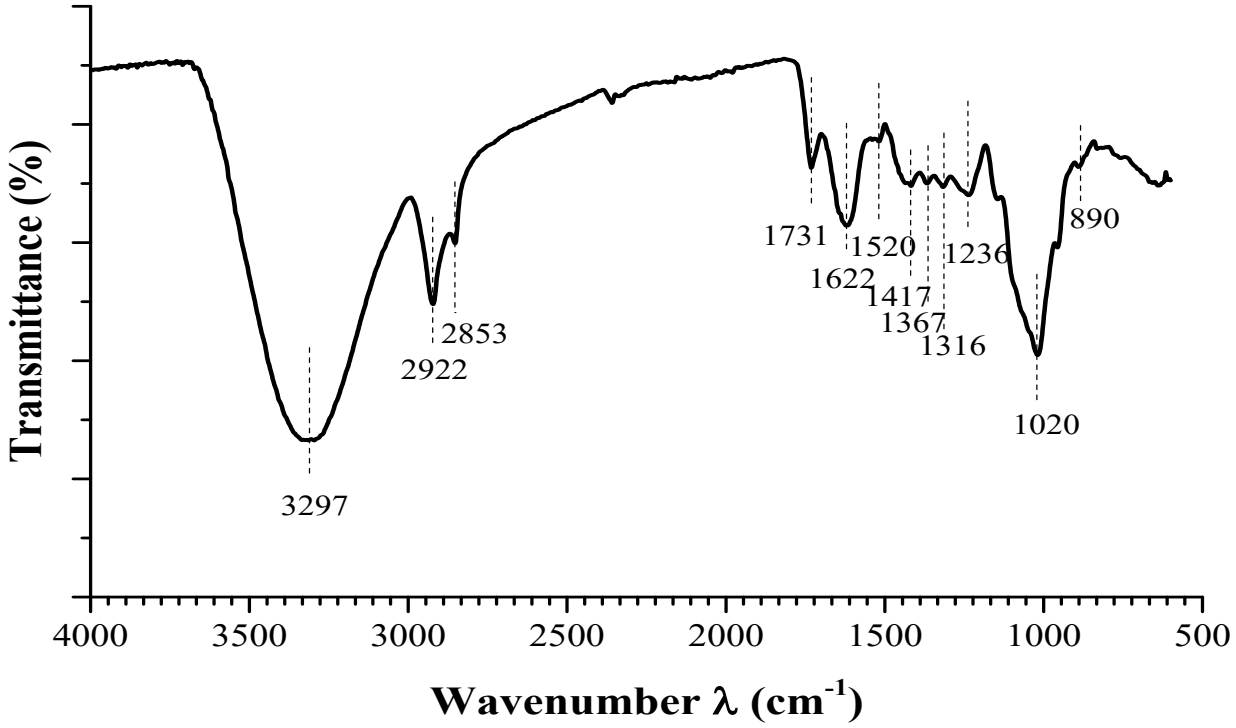

Figure S17. FTIR spectrum of undissolved residue obtained after polyphenols extraction with ChCl:EG.

Table S3. Main absorption bands and assignments related to the residue obtained after polyphenols extraction with ChCl:EG.

Absorption bands (cm^{-1})	Main Assignments	References
3297	stretching vibrations of the inter and intramolecular hydrogen bonds of the O-H group in cellulose, hemicellulose, pectin, and lignin	7–11
2922-2853	Symmetric and asymmetric stretching of C-H (in methyl and methylene groups) in hemicellulose/cellulose/pectin along with the aromatic ring vibration in lignin	
1731	C=O stretching of acetyl and uronic ester groups of hemicellulose or the ester groups of ferulic and *p*-coumaric acids of lignin or methyl esters in pectin	
1622	C=C deformation modes and stretching vibrations of lignin aromatic rings	
1520	C=C stretching vibrations of lignin aromatic rings	
1417	C=C deformation modes and stretching vibrations of lignin aromatic rings and C-H and O-H bending in carbohydrate fractions	
1367	CH_2 symmetrical vibration of cellulose/hemicellulose OH bending vibration of pectin	
1316	CH_2 wagging of cellulose	
1236	C-O stretching of syringyl rings, C-O stretching in lignin and hemicellulose and OH-plane deformation	
1020	C-O-C ring vibrational stretching modes of cellulose/hemicellulose/pectin glycosidic linkages	
890	β-glycosidic C-H deformation with a ring vibration contribution (hexoses/pentose) characteristic of glycosidic bonds	

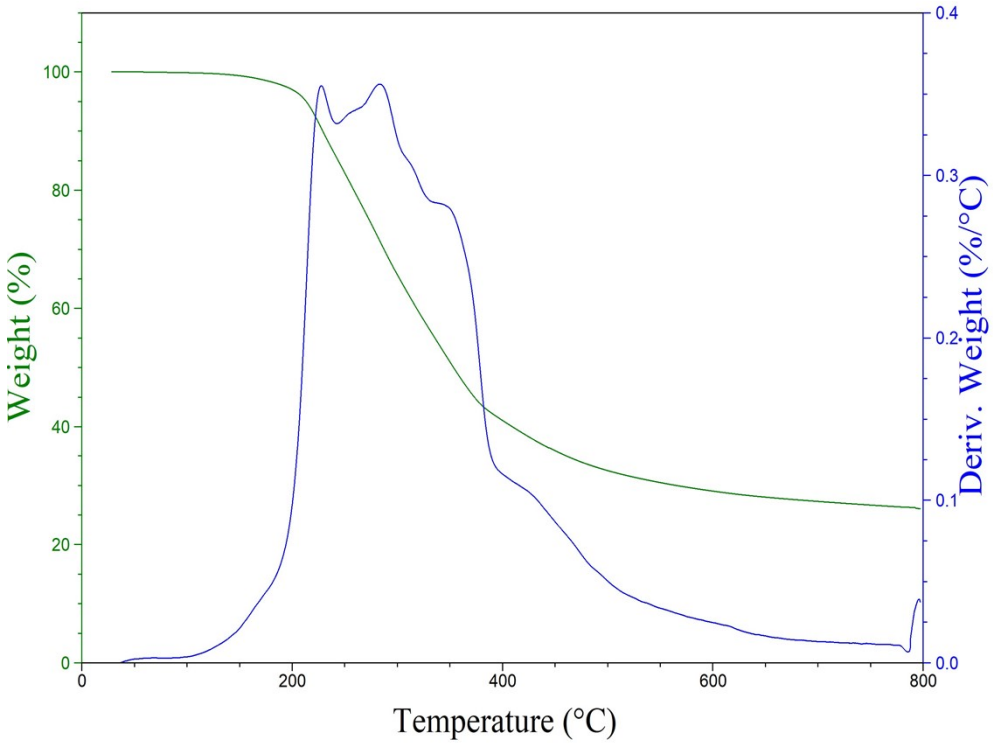

Figure S18. TG and DTG curves of undissolved residue obtained after polyphenols extraction with ChCl:EG.

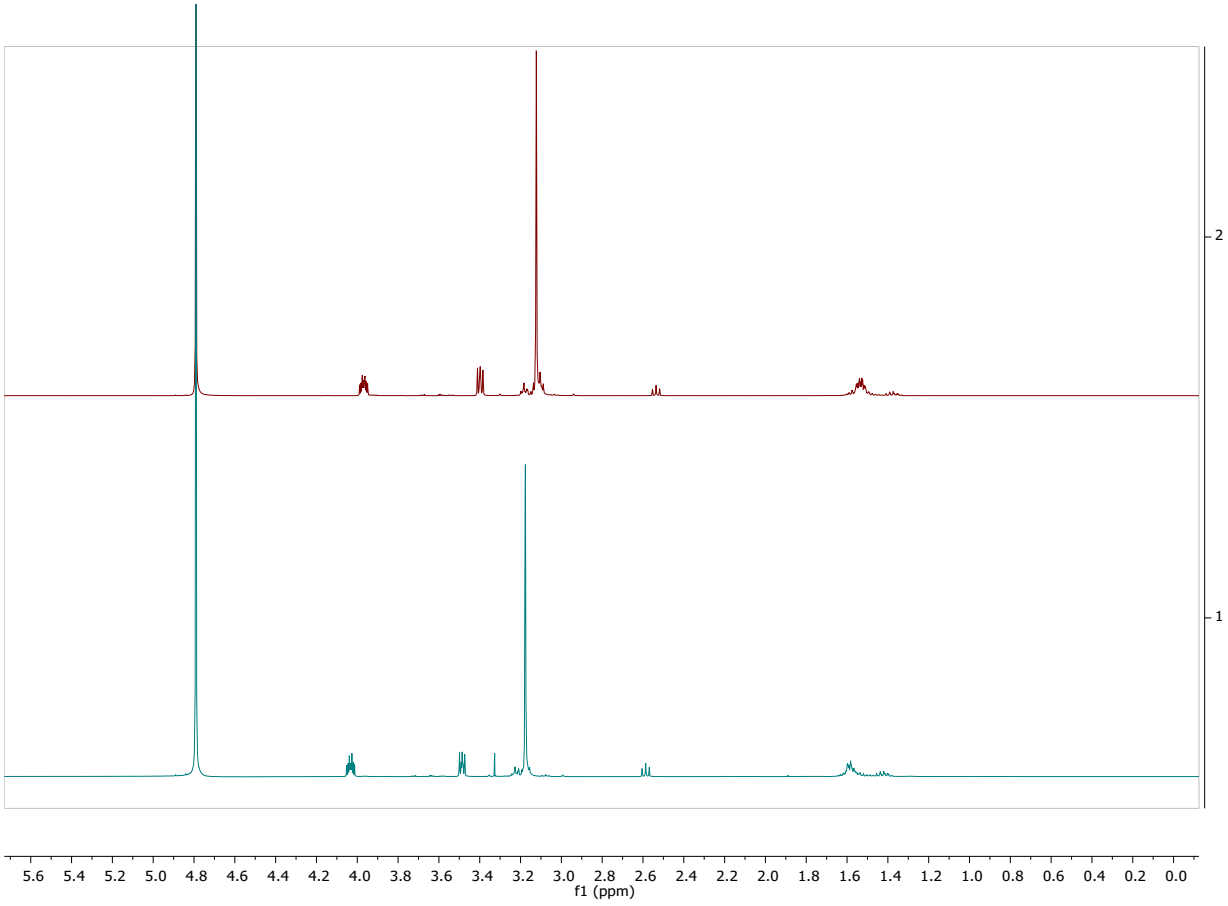

Figure S19. ^{1}H-NMR comparison of fresh (top) and recovered (bottom) ChArg bio-IL.

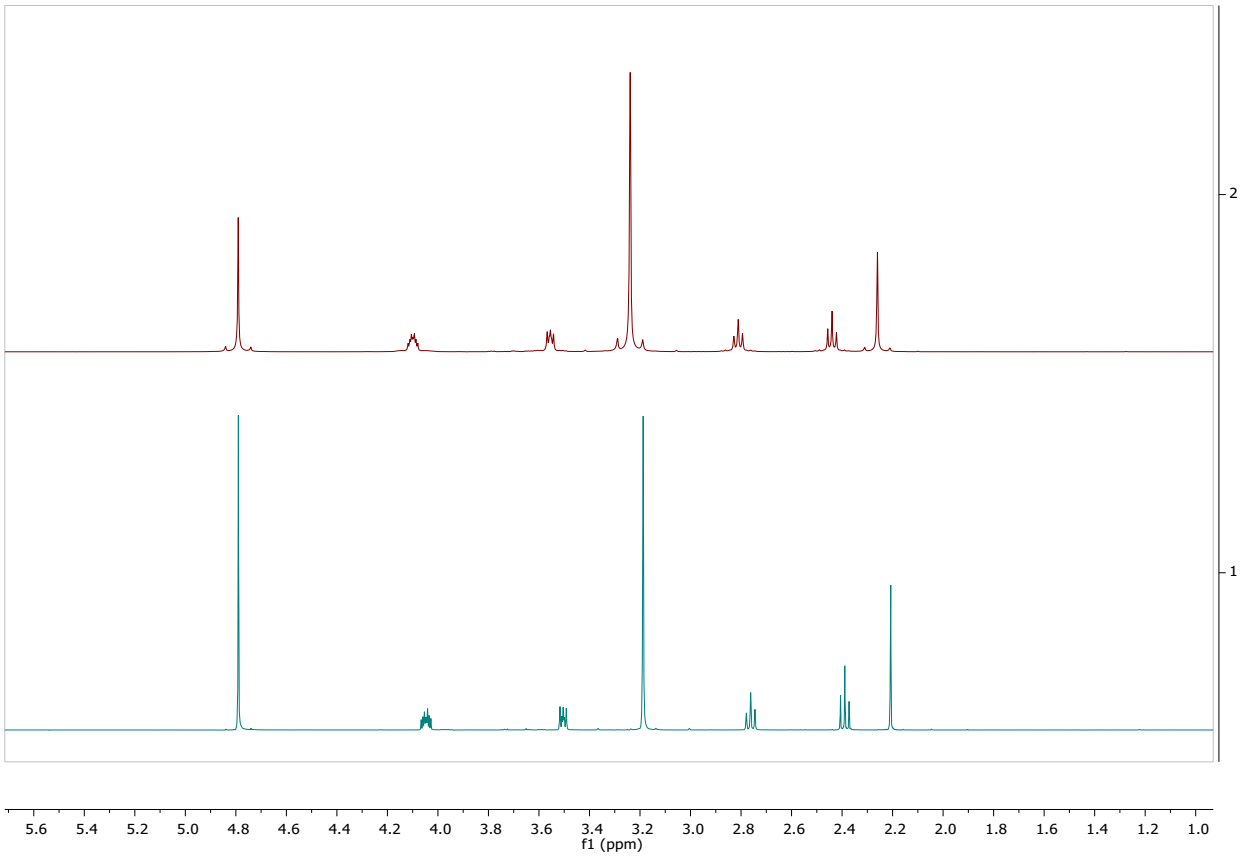

Figure S20. ^{1}H-NMR comparison of fresh (top) and recovered (bottom) ChLev bio-IL.

Table S4. Rheological data of ionogel extracted from frequency sweep test.

Ionogel - Frequency sweep			
Angular Frequency ω (rad/s)	**Storage modulus, G' (Pa), 25 °C**	**Loss Modulus, G'' (Pa), 25 °C**	**Complex viscosity η* (Pa·s), 25 °C**
100	16967	3051	172
63.1	16128	2799.1	259
39.8	15363	2571	391
25.1	14671	2358	591
15.8	14034	2167	896
10	13456	1999	1360
6.31	12928	1845.6	2070
3.98	12436	1711.2	3150
2.51	11986	1590.6	4810
1.58	11563	1495.8	7360
1	11166	1409.2	11200
0.631	10824	1347.6	17300
0.398	10495	1265.2	26500
0.251	10169	1225.4	40800
0.158	9900.4	1184.9	62900
0.1	9577.9	1172.6	96500

References

1 A. B. N. Saïed, M. Khelifi, M. Aider, *Trans. ASABE*, 2017, **60**, 253–261.

2 J.-S. Yang, T.-H. Mu and M.-M. Ma, *Food Chem.*, 2018, **244**, 197–205.

3 T. Yokoyama, J. F. Kadla and H. Chang, *J. Agric. Food Chem.*, 2002, **50**, 1040–1044.

4 M. M. Villar-Chavero, J. C. Domínguez, M. V. Alonso, M. Oliet and F. Rodriguez, *Carbohydr. Polym.*, 2019, **207**, 775–781.

5 R. Ranjan, K. Rawat and H. B. Bohidar, *Phys. Chem. Chem. Phys.*, 2017, **19**, 22934–22945.

6 M. Irani, S. M. A. Razavi, E.-S. M. Abdel-Aal, P. Hucl and C. A. Patterson, *Int. J. Biol. Macromol.*, 2019, **124**, 270–281.

7 A. Mero, N. R. Moody, E. Husanu, A. Mezzetta, F. D'Andrea, C. S. Pomelli, N. Bernaert, F. Paradisi and L. Guazzelli, *Front. Chem.*, 2023, **11**, 1270221.

8 R. Javier-Astete, J. Jimenez-Davalos and G. Zolla, *PLoS One*, 2021, **16**, 0256559.

9 F. Xu, J. Yu, T. Tesso, F. Dowell and D. Wang, *Appl. Energy*, 2013, **104**, 801–809.

10 A. Kozioł, K. Środa-Pomianek, A. Górniak, A. Wikiera, K. Cyprych and M. Malik, *Coatings*, 2022, **12**, 546.

11 M. Fasoli, R. Dell'Anna, S. Dal Santo, R. Balestrini, A. Sanson, M. Pezzotti, F. Monti and S. Zenoni, *Plant Cell Physiol.*, 2016, **57**, 1332–1349.